LA-UR-19-30861
Approved for public release; distribution is unlimited.

Title: PNAR Measurement Report

Author(s): Tobin, Stephen Joseph
Tupasela, Topi
Dendooven, Peter
Honkamaa, Tapani

Intended for: Report

Issued: 2019-10-25

PNAR Measurement Report

By Topi Tupasela, Stephen J. Tobin, Peter Dendooven, Tapani Honkamaa

Radiation and Nuclear Safety Authority

Steve Tobin

Contents

1 Introduction

STUK performed an NDA inspection at the spent fuel interim storage facility at Olkiluoto NPP during 22.7-26.7.2019. The inspection was also attended by experts from US DOE-LANL, Helsinki Institute of Physics, Euratom and IAEA and was made possible by the operators from TVO. The inspection included fuel verification with STUK's new PNAR instrument and IAEA's PGET. Simultaneous measurements were made possible with a support quadropod common for both instruments. The inspection and the results of the PGET verification are described in separate memorandums. This report focuses on the results of the PNAR verification.

The inspection was the very first one performed with STUK's PNAR instrument. Thus, the main goal of the inspection from the PNAR point-of-view was to demonstrate that the PNAR method works in practice, identify possible improvements and assess if PNAR can be utilized in SNF verification. Furthermore, the measurement campaign was an initial step in exploring the fuel parameter range where PNAR could be used and an initial investigation into quantifying the uncertainties of the system.

2 Measurement setup

2.1 Equipment

The final PNAR design and the PNAR method are described in [1]. The complete measurement setup is shown in Figure 1. The main measurement principle in this implementation of PNAR, is to measure relative fast neutron count rates in high- and low-multiplying measurement configurations. The high-multiplying configuration features the measured fuel assembly surrounded by enough reflecting medium (water of the storage pond and polyethylene) so that neutron albedo is relatively elevated. The low-multiplying configuration is achieved by moving a cadmium liner in between the fuel assembly and the PNAR instrument to suppress the neutron albedo. The liner is positioned as close to the fuel assembly as possible, leaving most of the reflecting media outside. The ratio of these two measurements is defined as the PNAR Ratio, which is proportional to the neutron multiplication in the fuel, which is in turn caused by the presence of fissile material. In addition to the fast neutron detectors, PNAR houses four ionization chambers to measure gross gamma radiation.

The PNAR instrument features four identical, independent detector pods arranged into a square as viewed from above while leaving an opening in the middle where a fuel assembly is lowered in. A picture from the construction phase is shown in Figure 2 where the pod identification can be seen. The pods are labelled as 1-4 in a counter clockwise order as viewed from above. At the start of the measurements, the cable connection chamber of pod 3 was identified as leaking. Thus, only pods 1,2 and 4 were used throughout the week.

One design requirement for the PNAR instrument was a measurement time of 5 minutes, consisting of two 2-minute measurements (1 in each configuration) and 1 minute reserved for repositioning of the cadmium liner and data management. Due to

constraints caused by the measurement software, the total measurement time was increased to 2x3 minutes to ensure that 2 minutes worth of counts were saved from all independent measurements. The time needed to move the manually operated cadmium liner was 5-10 seconds. The liner moved along the central channel and into the opening in the PNAR smoothly and the top and bottom positions were easily identified by the person moving the liner. The liner stayed in the top position when the lifting chain was bent over the railing at the edge of the pool. Additionally, the position of the liner was followed with an underwater camera.

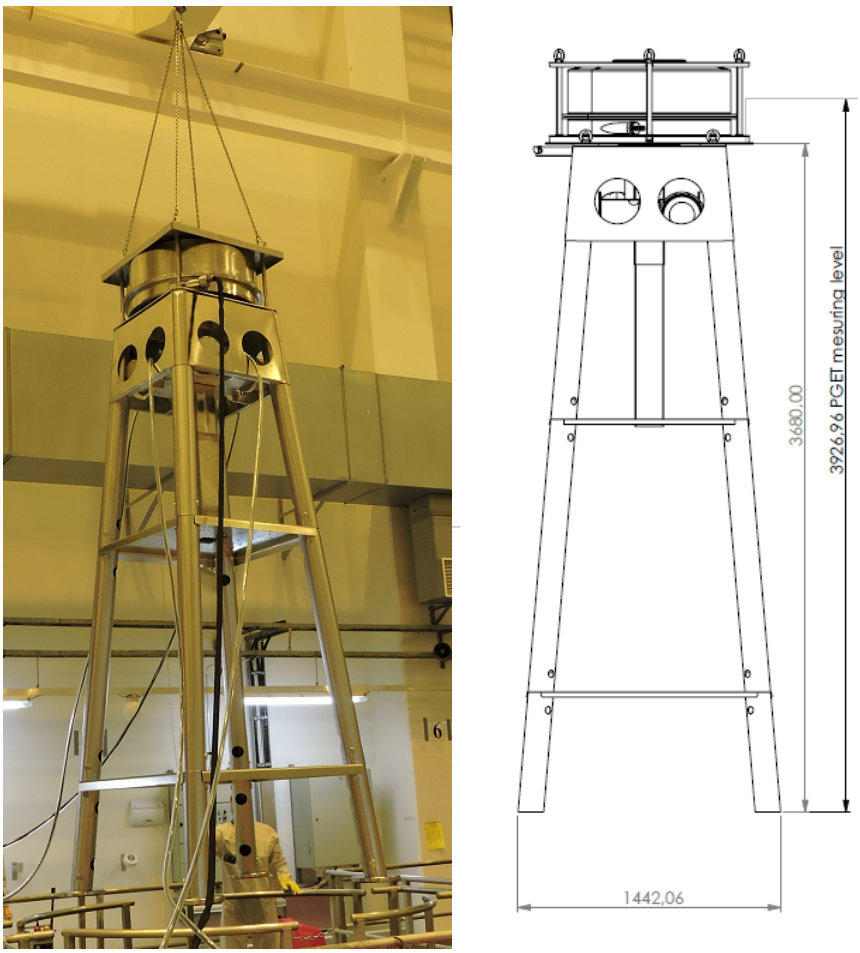

Figure 1: Left: Measurement equipment being hoisted out of the fuel pond. Picture from TVO. Right: Drawing of the measurement system. PGET sits on top of the support quadropod and PNAR is positioned below it. The support is 3.7m tall to allow for measurements from any height of a fuel assembly.

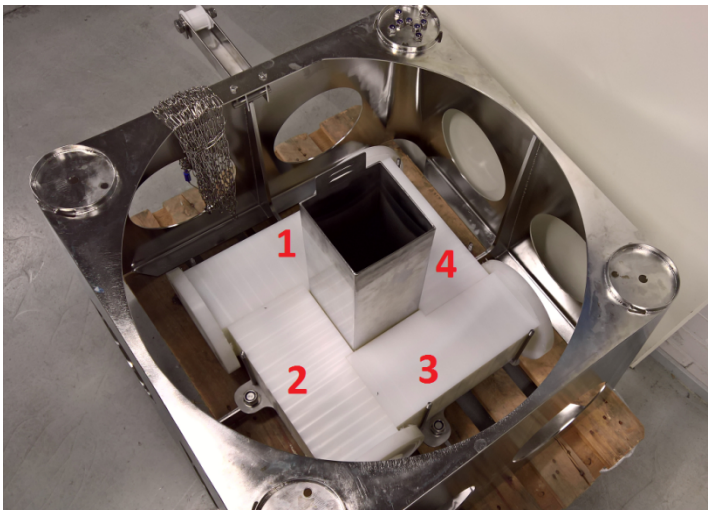

Figure 2: Modular design of the PNAR instrument around the cadmium liner. The indicated pod numbering is used throughout this report.

The centre channel was designed to follow the dimensions of a spent fuel storage rack (150 mm x 150 mm central opening). However, the final channel was tighter than designed. The dimensions of the final channel were measured at 100 mm intervals along all its sides. The tightest spot was near one side at the neck of the channel with an internal width of 146 mm. Along the channel, the external width ranged between 152 and 155 mm. The channel is made of 3 mm thick steel. The channel bulged along the two weld seams, which was one of the causes for the smaller inner dimensions. Regardless of the smaller-than-designed dimensions, all measured assemblies fit inside the centre channel.

The cadmium liner consists of cadmium sandwiched between two 550 mm long, 1.2 mm thick stainless steel sheets. The cadmium layer is 500 mm long, centered in the liner, 1 mm thick in the middle of each side and 0.5 mm thick in the corners. The enclosed liner has a small bow, making it slightly larger near the bottom end. Furthermore, the liner has slightly bulged outwards along the two vertical welding seams. The largest outer measures of the liner are 168 mm x 166 mm located near the bottom end of the liner, while the dimensions are 166 x 166 mm at the middle of the liner. Inside measurements were taken at the ends of the liner. These range between 158 mm and 159 mm.

2.1.1 Electronics

Table 1: Serial numbers of the detectors used in each detector pod.

Pod	Preamplifier	Neutron detector	Gamma detector
1	1817503	18E00WYA	877060
2	1817504	18E00WY8	871650
3	1817501	18E00WY9	877044
4	1817502	18E00WYE	877037

The measurement electronics include four SMC 2100-IFI-CNT units by FST, each controlling one ^{3}He-tube and gamma detector in one detector pod. The control units are the same as those that are used with Fork detectors by the European Commission (EC). The units are connected in a serial network and controlled with AM-SMCA01 software by FST through a single laptop PC. Separate counting units for each detector pod means independent measurements from all pods, but the units had to be controlled separately making starting and stopping measurements slow. Furthermore, a time lag was noticed when saving data from very short measurement intervals (e.g. a single 5 s measurement took 15 s in total before the next one started). The cause for this delay remained unidentified. A compromise of leaving the detectors running for the whole day in 15 second counting intervals was made. For future reference, the detectors used in each pod are identified in Table 1.

Figure 3 shows the cables coming from the pool and the control units connected to a laptop. The cables of the pods were too short and the cables barely reached the surface of the pool. New ones must be assembled before the next campaign.

Bias voltage of (-)500V was selected for the gamma detectors. The decision was made based on the fact that the detectors were tested with this bias. It should be noted that high gamma radiation may cause the detectors to measure in the non-linear regime even with this bias. However, the gamma measurements were a low priority in this campaign.

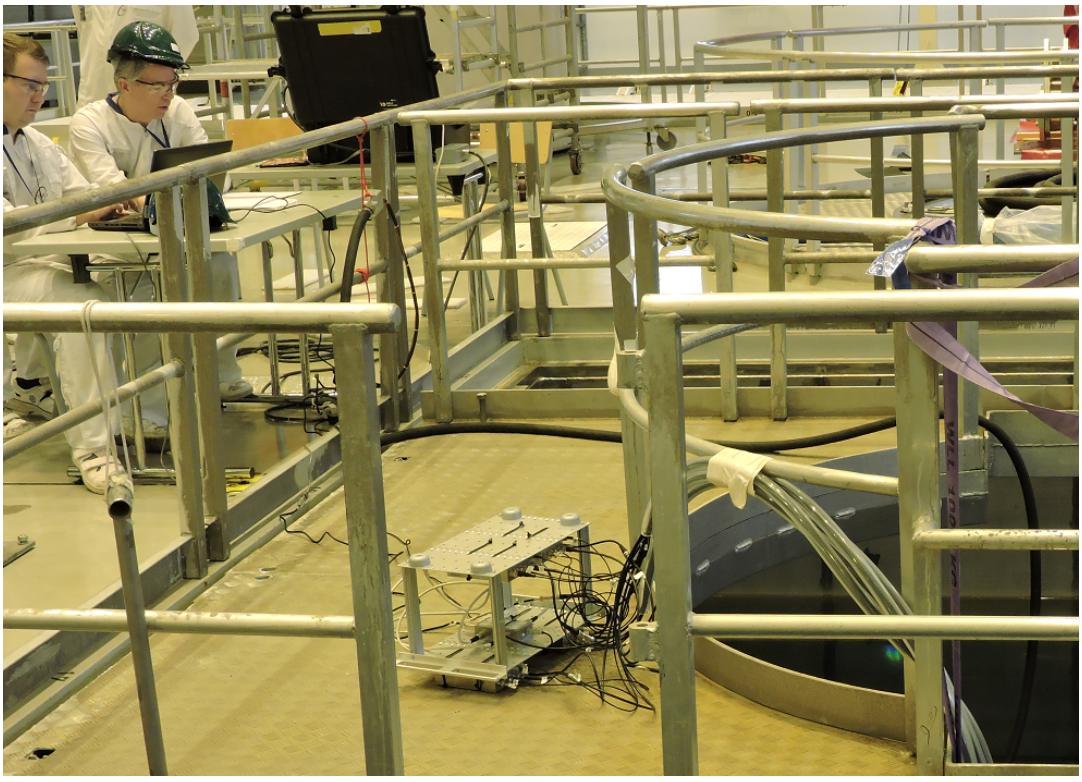

Figure 3: Detector controller units poolside. The units are connected to a laptop with a single USB. Picture: TVO.

2.1.2 Neutron detector bias

The PNAR was designed to verify fuel that was cooled for at least 20 years after discharge. To select the bias for neutron detectors for all of the measurements, a bias voltage scan was performed with an assembly that was estimated to have the highest gamma radiation in the PNAR measurement range. The selected assembly had an IE of 3.231%, a BU of 37107 MWd/tU and a 17.2 years of cooling time. The scan results are plotted in Figure 4. Based on the location of the plateau in the scan, a bias voltage of 1560 V was selected for all neutron detectors; this voltage was selected (a) because the count rate does not change significantly with variation in the bias voltage, thus reducing sensitivity to this variable and (b) 1560V is below the level at which gamma rays first start to have an impact on the count rate, which appears to start around 1600 V in Figure 5. Later, a voltage scan was also performed on the hottest assembly measured during the week (IE 3.521, BU 43312, CT 6.2). The results are plotted in Figure 5. The detectors seem to work in the linear regime even with such hot assembly, even though the internal lead shielding was not designed to suppress such high gamma flux enough to not interfere with the neutron detectors. For reference, the measured gross gamma count rate was approximately 2 times higher for the hottest assembly in respect to the one the calibration was made with.

In preliminary testing, a factorial dead time of 6 % at 50 000 cps, when operating with 1600 V bias voltage, was estimated for the neutron detectors. As the PNAR Ratio is a division between two count rates with very similar dead time effect and as the dead time is estimated to have only a small effect at the measured count rates, dead time correction was neglected in further analysis. The counting software does no dead time correction.

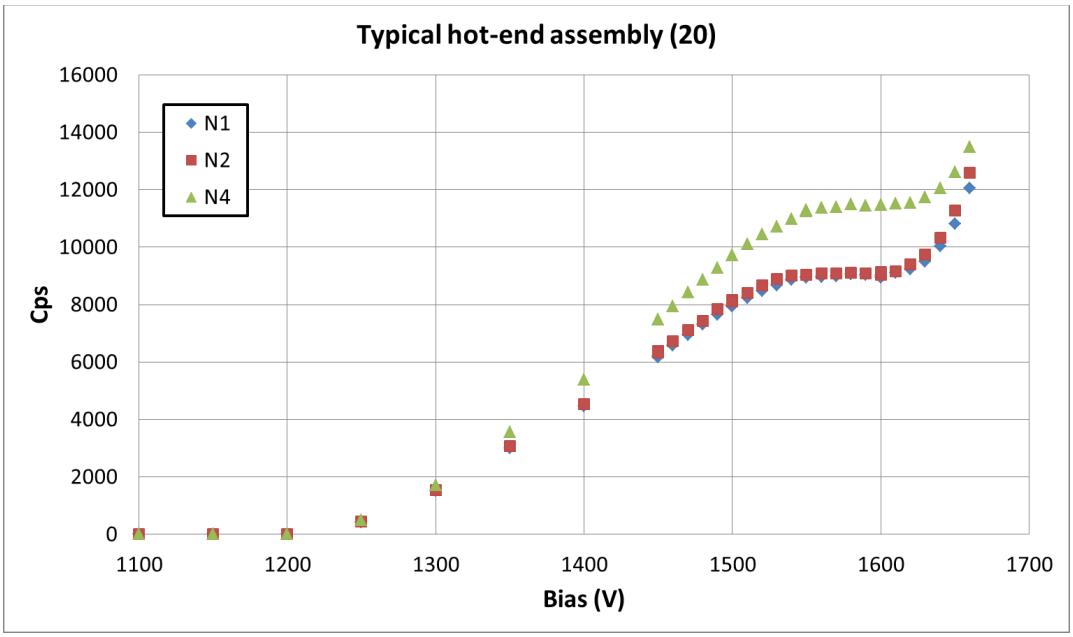

Figure 4: Bias voltage scan of an assembly from the hot end of PNAR measurement range. (Assembly #20) N1-4 refer to neutron detectors in pods 1-4, respectively.

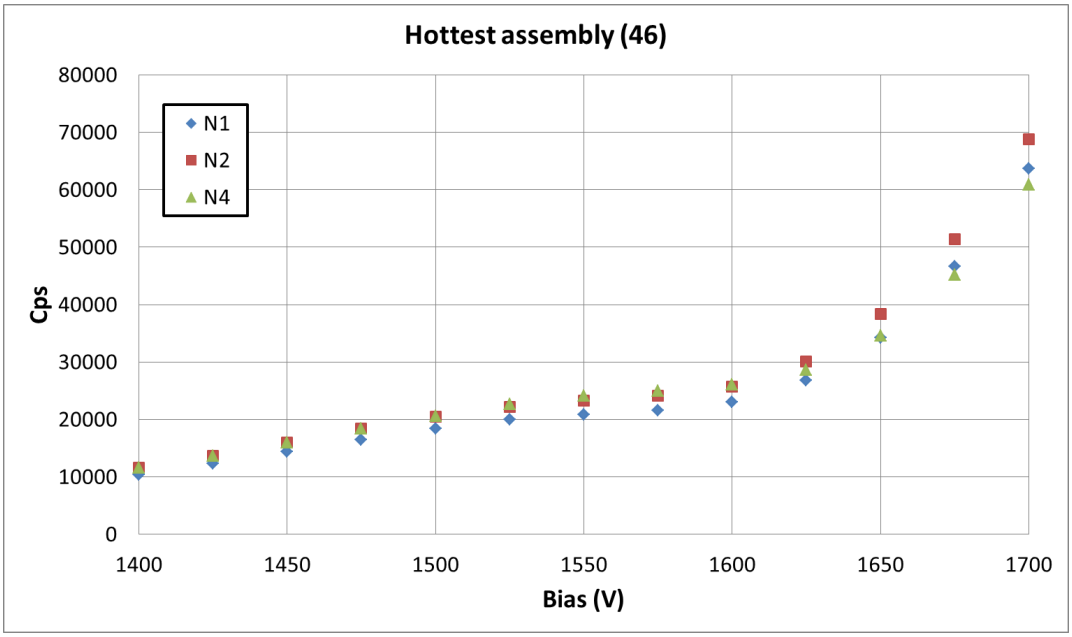

Figure 5: Voltage scan on the hottest measured assembly. A small plateau is still present around the selected bias of 1560V. (Assembly #46)

2.2 Inspected assemblies

A total of 23 different assemblies were inspected. The inspected assemblies included several different assembly designs including ones with partial length rods. Cooling times ranged from 6.2 years to 35.1 years, where the oldest one was from the initial reactor core making it an interesting assembly from a calibration point of view, as it has a low average enrichment and burnup. The burnups ranged from 18589 MWd/tU to 49698 MWd/tU. All the assembly parameters are listed in

Table 3. All the assemblies were measured from a default measurement height, at approximately 1.4 meters from the bottom of the assembly to the axial midpoint of the PNAR instrument, which is also where the neutron detectors are located. Depending on the assembly design, there is approximately 0.4 meters of support structures and natural uranium at the bottom of the assembly before enriched uranium. In addition to the default height measurements, several assemblies were measured at 1.5 m above the default height and one assembly was measured at 7 different heights. Several assemblies were measured multiple times after rotating the assembly 90 degrees between each measurement. Figure 6 shows an assembly being measured.

2.3 Non-multiplying object

Before the inspection measurement campaign, the PNAR Ratio of a non-multiplying object was measured at STUK. The measurement was done by lowering the PNAR into a $1m^3$ water tank and placing a Cf neutron source into the centre of the central opening of the PNAR. The measurement was repeated with and without the cadmium liner. One cable was identified to be broken (in pod 2) during the measurement and was fixed before the inspection. The individual count rates measured are listed in Table 2. The cumulative count rates from two opposite side detectors (1 and 3) were 48632 cps with Cd liner and 45703 cps without the Cd liner, resulting into a PNAR Ratio of 0.940. As the Cd liner displaces water, the PNAR Ratio is lower than 1 when measuring neutron radiation without multiplying material present. The measurements were performed only once and it should be noted that because the whole center opening was filled with water around the 20 mm diameter source, the energy spectrum of the neutrons did not accurately represent that of a spent fuel. Therefore, the result should be viewed critically. MCNP simulations have shown, that lower energy neutrons result into lower PNAR Ratios in this PNAR configuration.

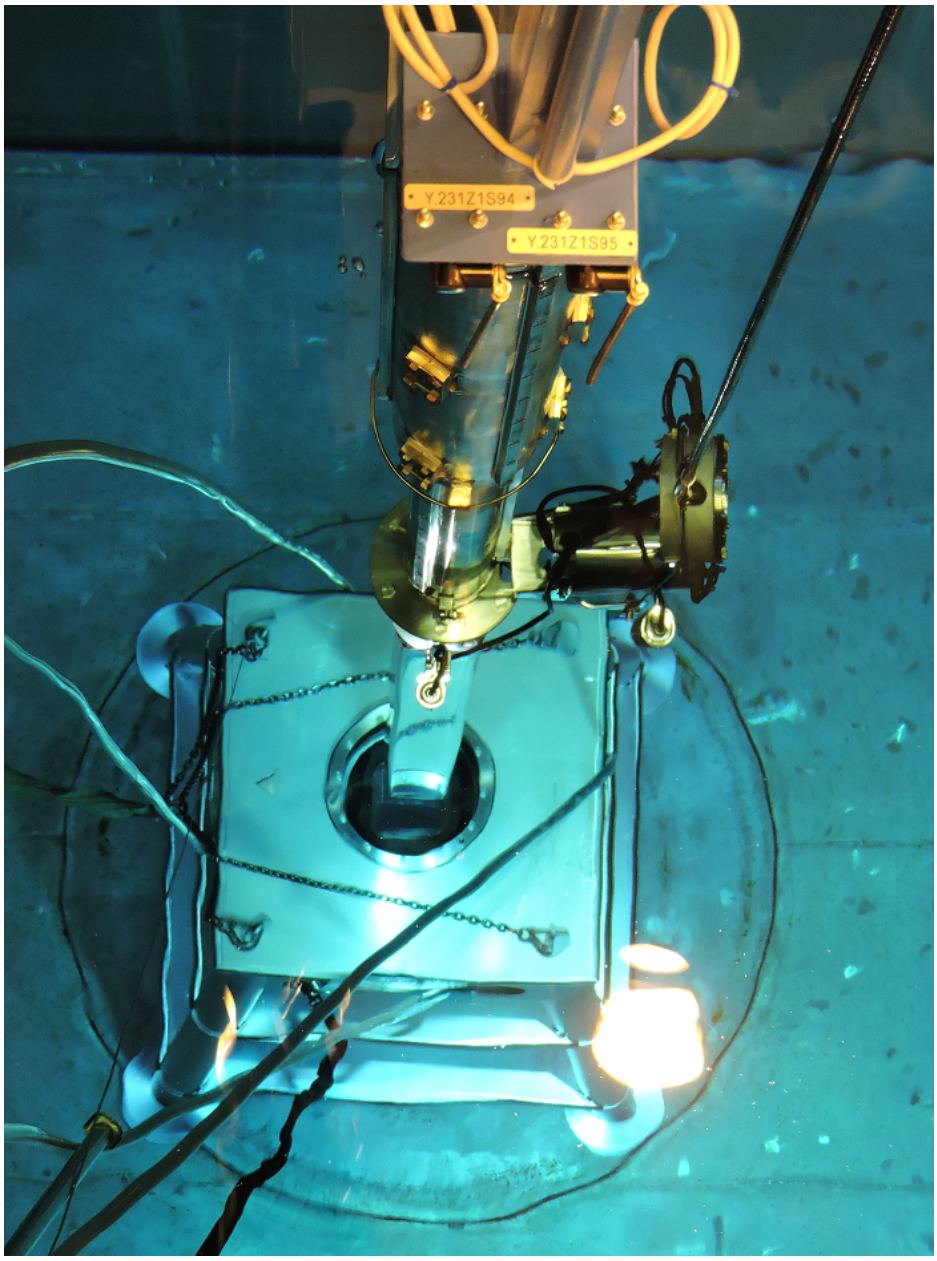

Figure 6: A fuel assembly in the measurement position. Picture: TVO.

Table 2: Pod-specific count rates in the non-multiplying object measurement.

	Pod 1	Pod 3	Pod 4	Pods 1+3
CPS with Cd	24797	23834	24263	48632
CPS without Cd	23756	21947	22560	45706
PNAR Ratio	0.958	0.921	0.930	0.940

3 Results and discussion

3.1 PNAR Ratios and gross count rates

Table 3 identifies all the measured assemblies. Throughout this report, assemblies are referred to with their id #. To reduce positional uncertainty (i.e. the error raising from the fact that the fuel, the Cd liner and the PNAR are not necessarily in the same positions relative to each other between measurements), the PNAR measurements are expected to be averaged over the four pods. Since pod 3 was not functioning during the measurements, the PNAR Ratios stated in

Table 3 are calculated using the two functioning opposite pods 2 and 4. The given standard deviation is calculated from counting statistics. (i.e. square root of the total counts) Other sources of uncertainty are discussed in Section 3.2.

Based on MCNP simulations, the PNAR Ratio of a non-multiplying assembly is expected to be 0.9800. The PNAR Ratio of the assembly with the lowest neutron count rate (#1), thus assuming counting statistics are the dominant uncertainty for this extreme low count rate case, differs from the non-multiplicating PNAR Ratio by 24 standard deviations.

Table 3: Inspected assemblies and the measured PNAR Ratios and gross count rates from the default measuring position. PNAR Ratios and gross count rates are averaged over two opposite detector pods (2 and 4). The reported standard deviation is only due to counting statistics.

Assembly #	Assembly type	IE (%)	BU (MWd/tU)	CT (a)	PNAR Ratio	PNAR stdev. (±)	Neutron cps	Gamma cps
1	8x8-1	1.938	18589	35.1	**1.0422**	**0.0026**	700	92740
2	8x8-1	2.907	31161	29.1	**1.0397**	**0.0017**	3190	176222
3	SVEA-64	2.975	33994	21.2	**1.0427**	**0.0011**	7777	279365
4	SVEA-64	2.975	37574	21.2	**1.0443**	**0.0009**	10789	298479
5	SVEA-64	2.976	19770	23.2	**1.0883**	**0.0032**	970	163324
6	SVEA-64	2.98	32988	20.2	**1.0492**	**0.0011**	7195	278921
11	SVEA-64	2.992	32935	21.2	**1.0476**	**0.0012**	6767	271823
13	SVEA-64	3.015	35672	21.2	**1.0451**	**0.0010**	9322	293573
18	9x9-1AB	3.224	35399	23.1	**1.0376**	**0.0012**	6349	246719
20	ATRIUM10	3.231	37107	17.2	**1.0495**	**0.0009**	10250	312880
22	SVEA-100	3.235	37604	19.2	**1.0441**	**0.0010**	8740	300604
23	SVEA-64	2.975	33919	21.2	**1.0445**	**0.0010**	8517	281565
24	SVEA-64	2.976	33175	21.2	**1.0445**	**0.0010**	6473	270442
28	SVEA-64	2.989	32581	21.2	**1.0465**	**0.0010**	6230	251004
30	9x9-1AB	3.22	35043	21.1	**1.0457**	**0.0012**	6246	253222
31	9x9-1AB	3.226	35884	21.1	**1.0423**	**0.0012**	6084	251833
35	Optima	3.192	39758	14.2	**1.0464**	**0.0008**	15694	394146
39	ATRIUM10	3.22	35039	17.2	**1.0536**	**0.0011**	7796	292990
42	GE12	3.237	36281	17.2	**1.0453**	**0.0011**	8771	304521
43	GE12	3.245	43088	12.2	**1.0386**	**0.0006**	18451	401907
44	GE14	3.463	42159	10.2	**1.0443**	**0.0007**	20794	472094
46	GE14	3.521	43312	6.2	**1.0490**	**0.0006**	23963	653852
49	ATRIUM10	3.554	49698	8.4	**1.0306**	**0.0005**	30164	492139

The majority of the PNAR Ratios falls between 1.03 and 1.05. Assembly #5 stands out with a PNAR Ratio of 1.088. This assembly has a relatively low burnup compared to its IE (i.e. it is not fully burned). Therefore, it has more ^{235}U left and the accumulated Pu has fractionally more fissile ^{239}Pu than a fully burnt assembly would have. Compared to the other measured assemblies, it has more fissile content which is also indicated by the PNAR Ratio. The average PNAR Ratio of the assemblies other than #5 is 1.044.

The preliminary simulations [2] estimate a PNAR Ratio of 1.109±0.003 for an assembly with IE 3%, BU 30000 MWD/tU and CT 20 a and 1.147±0.003 for a similar assembly with BU of 15000 MWD/tU. The difference between these PNAR Ratios is 3.4 %, while the difference between similiar measured assemblies #5 and #28 is 4.0% even though the burnup-difference is smaller than between the simulated assemblies. The measured

PNAR Ratios are systemically lower than simulated ones, but the relative difference between the one half-burned assembly and the rest is larger.

3.1.1 Pod-specific PNAR Ratios

By using independent counting electronics for each pod, it is possible to measure separate PNAR Ratios from all pods, each more sensitive to the fuel pins and the water gap closest to the selected pod. Tables 4-7 show pod-specific PNAR Ratios of assemblies #28, #18, #24 and #42, respectively. The rows in the table are different measurements. All of these measurements were made on the default measurement height. The background colours in the tables indicate the same side of the fuel assembly as the assembly was rotated between measurements. Especially from assembly #18, it can be seen that measurements from two sides of the assembly (white and green) result in significantly lower PNAR Ratio than the other two (blue and red). This effect is consistent through all rotations of the fuel, meaning that it cannot be caused by inhomogeneity between pods or sides of the Cd liner. Thus, it means angular anisotropicity in the fuel.

In the BWR reactor this fuel is from, cross-shaped control rods are used between sets of four assemblies. Thus, two sides of each assembly have been exposed to a control rod and two have not. It is possible that the different neutron flux between these two areas have resulted into variance in the remaining content of fissile material. However, this is usually compensated by having lower initial enrichment in the pins on the control rod side than on the opposite side. As the use of control rods varies between different areas in the core and the cycle history varies between assemblies, the effect is different for each assembly.

Table 4: Pod-specific PNAR Ratios of assembly #28. The background colors indicate the same side of the assembly. The default position was measured four separate times and the assembly was rotated to measure once from all sides with each detector. The reported uncertainties are counting statistics based standard deviations.

Pod 1	Pod 2	Pod 4	Pods 2+4
1.0439±0.0015	1.0529±0.0015	1.0401±0.0015	1.0465±0.001
1.0468±0.0016	1.0535±0.0016	1.0434±0.0016	1.0483±0.0011
1.0454±0.0017	1.053±0.0017	1.0405±0.0017	1.0468±0.0012
1.039±0.0013	1.0547±0.0013	1.0445±0.0014	1.0503±0.001
1.0436±0.0016	1.0409±0.0015	1.0611±0.0016	1.051±0.0011
1.0473±0.0017	1.0451±0.0017	1.0509±0.0015	1.0481±0.0011
1.0443±0.0017	1.051±0.0017	1.0418±0.0017	1.0464±0.0012

Table 5: Pod-specific PNAR Ratios of assembly #18.

Pod 1	Pod 2	Pod 4	Pods 2+4
1.0538±0.0019	1.0532±0.0019	1.0258±0.0016	1.0376±0.0012
1.0283±0.0017	1.0575±0.0018	1.0246±0.0016	1.0401±0.0012
1.0272±0.0016	1.0296±0.0015	1.0528±0.0018	1.039±0.0012
1.055±0.0019	1.0244±0.0016	1.0613±0.0019	1.0407±0.0012
1.0569±0.0019	1.0506±0.0019	1.0296±0.0016	1.0385±0.0012

Table 6: Pod-specific PNAR Ratios of assembly #24

Pod 1	Pod 2	Pod 4	Pods 2+4
1.049±0.0016	1.0508±0.0016	1.0394±0.0014	1.0445±0.001
1.0336±0.0016	1.0503±0.0018	1.0411±0.0016	1.0454±0.0012
1.0339±0.0016	1.0371±0.0015	1.0546±0.0017	1.0448±0.0011
1.0517±0.002	1.0372±0.0018	1.0529±0.0021	1.044±0.0013
1.0503±0.0018	1.0533±0.0018	1.0394±0.0016	1.0456±0.0012

Table 7: Pod-specific PNAR Ratios of assembly #42

Pod 1	Pod 2	Pod 4	Pods 2+4
1.0458±0.0016	1.0492±0.0016	1.042±0.0015	1.0453±0.0011
1.034±0.0013	1.0525±0.0013	1.0371±0.0013	1.0446±0.0009
1.0342±0.0013	1.0367±0.0013	1.056±0.0014	1.046±0.001
1.049±0.0015	1.0369±0.0014	1.0559±0.0015	1.0461±0.001
1.047±0.0014	1.0489±0.0014	1.0418±0.0013	1.0452±0.0009

The default measurement orientation of an assembly was always the same. Comparison of the PNAR measurement results to the PGET results indicates that the control rod facing sides of an assembly were blue and red. The average PNAR Ratios of the control blade facing pod pair and the opposing one are compared in Table 8. Assembly #28 had two replaced pins near one of the edges (both after 2 of 4 cycles), which might affect the PNAR Ratio of the nearest pod. All assemblies show a difference in average PNAR Ratios between the two pairs. In all four examined cases, the corner with lower PNAR Ratio is the one facing the control blade – assuming that the matching of PNAR and PGET data is correct.[1]

[1] This was made by following a missing pin in the PGET sinogram, while knowing the initial position of the detectors, the rotation direction and the detector indexing. The control blade position was identified from an asymmetrically positioned water channel.

Table 8: Average PNAR Ratios per side of fuel assembly for all rotated measurement series and the average PNAR ratios between the two pairs of sides assumed to be facing and not facing the control blade (bolded).

Assembly	Blue	Red	Green	White
#18	1.0574	1.0529	1.0283	1.0254
	1.0551		**1.0268**	
#28	1.0477	1.0531	1.0410	1.0444
	1.0504		**1.0427**	
#24	1.0506	1.0526	1.0374	1.0374
	1.0516		**1.0374**	
#42	1.0503	1.0508	1.0386	1.0361
	1.0505		**1.0374**	

3.1.2 Axial variation

The effect of measurement height was studied by measuring assembly #4 from 7 different heights. The lowest measurement was done on the very bottom of the assembly and resulted into a PNAR Ratio of 1.10. This measurement was likely biased by the fact that the fuel rods ended in the region PNAR is sensitive to. Furthermore, the count rates measured were very low, increasing statistical uncertainty. This measurement point is neglected in further analysis. For the remaining 6 measurements, the axial distance between the end of the enriched part of the active length of the assembly and the location of the neutron detectors was estimated to be at least 50 cm.

It is interesting to note that the BWR fuel is irradiated with an axial neutron energy gradient along the length of the fuel because the amount of water inside the assembly decreases from bottom to top. Yet, when the PNAR Ratio is measured, the amount of water is constant at all axial locations. Thus, when the fuel is irradiated the neutrons are on average higher in energy from top to bottom; while, when the fuel is measured, the neutron energy spectrum is essentially the same in all cases. Hence, a variation in the PNAR Ratio along the axial length of the fuel is not surprising. Detailed axial simulations of the irradiation and PNAR measurement are needed to better understand the observed trend.

The PNAR Ratios and gross gamma and neutron count rates (without cadmium liner) are reported in Figure 7. The gross count rates are normalized to the average count rate of all measurements. Measurement position “0” is the default position and the other heights are relative to it.

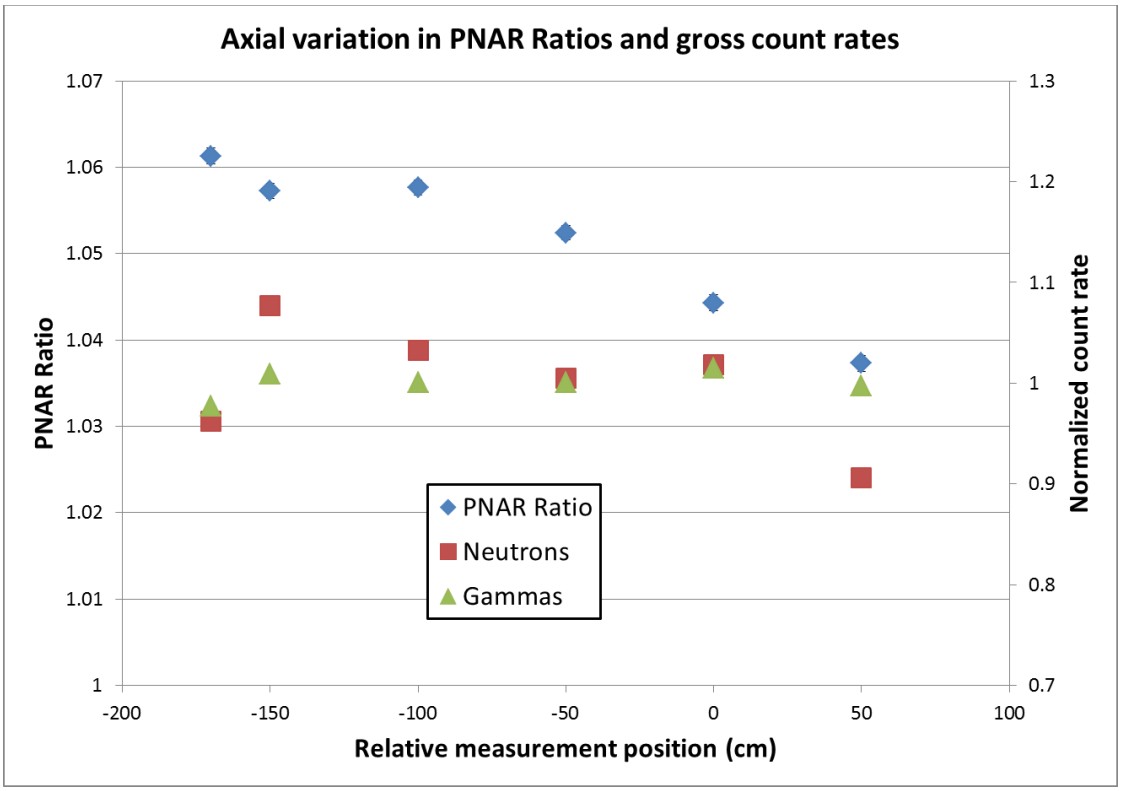

Figure 7: PNAR Ratios and gross neutron and gamma count rates at different measurement heights of assembly #4. The measurement position is relative to the default measurement height. The top of the assembly is on the left side. The count rates are normalized to the average count rate. All values are averaged from pods 2 and 4. The PNAR Ratio error bars (counting error) are partially hidden by the markers.

Gamma radiation is quite similar at all measured heights. Neutron radiation increases towards the top of the assembly. This is caused by the decreasing moderator density during burn which influences the accumulation of ^{244}Cm in the fuel. Also, the PNAR Ratio increases towards the top of the assembly, indicating increase in the fissile material content. This is likely also caused by the changing moderator density. At the highest measurement position, neutron radiation drops quickly while the PNAR Ratio does not. This indicates smaller fissile material depletion at the top of the assembly, where burnup is also lower.

In addition to assembly #4, 8 other assemblies were measured from two axial positions; from the default height and 150 cm above it. Unlike #4, all of these assemblies had partial length rods in them. Table 9**Error! Reference source not found.** summarizes the PNAR Ratios measured from these assemblies together with the change in neutron count rate between the positions. Assembly #4 had a relative change of +1.24 % in PNAR Ratio and +5.78 % in neutron count rate between the 0 and -150 cm measurements.

Unlike with assembly #4, the majority of these assemblies shows a drop in gross neutron count rate between the two measurement heights. Furthermore, only 3 of the assemblies

show a significant >0.5% change in PNAR Ratio. Compared to assembly #4, all of these assemblies are of newer, more complex designs. The difference compared to assembly #4 may be caused by more optimal fuel usage.

Table 9: PNAR Ratios and their differences between two measurement heights.

Assembly #	0 cm PNAR Ratio	-150 cm PNAR Ratio	Abs. PNAR Ratio difference	Rel. PNAR Ratio difference	Difference in neutron cps
20	1.0495	1.0531	0.0036	0.35 %	-9.15 %
39	1.0536	1.0534	-0.0001	-0.01 %	1.00 %
49	1.0306	1.0394	0.0088	0.85 %	-21.86 %
35	1.0464	1.0631	0.0167	1.60 %	-35.59 %
42	1.0452	1.0436	-0.0016	-0.15 %	-20.56 %
43	1.0386	1.0372	-0.0014	-0.13 %	-18.27 %
44	1.0443	1.0496	0.0053	0.50 %	-32.46 %
46	1.0490	1.0508	0.0018	0.18 %	-23.69 %

3.2 Uncertainty

The dynamic range of a PNAR Ratio measurement is influenced by the uncertainty in a single measurement. One of the main goals of the campaign was to quantify uncertainties in the instrument. The examined uncertainties were statistical uncertainties caused by the random nature of a counting measurement and the uncertainty caused by changes in the positioning of a fuel assembly relative to the Cd liner and to the detector. Note, that for the experimentally calculated PNAR Ratio, these two uncertainties are not separated. Additionally, the effect of accidental vertical mispositioning of the Cd liner was studied.

3.2.1 Counting statistics

The lowest measured count rate, when adding detectors 2 and 4 together, was approximately 1300 cps for the initial core assembly. Assuming a 2 minute measurement time, the counting uncertainty would be 0.25 %. At final verification, count rates of as low as 800 cps for all 4 detectors combined are expected, leading to an uncertainty of 0.32 %. Through propagation of error, such uncertainty leads to a relative standard deviation of 0.45 % in the PNAR Ratio. To reduce the uncertainty caused by counting statistics, longer measurement times may be needed for the longer cooled assemblies. However, the majority of the deposited assemblies are expected to have significantly higher count rates comparable to the 20 years cooled assemblies measured during the campaign, for which the error in PNAR Ratios were approximately 0.1 %. In the future, all four pods are expected to be used effectively doubling the total counting rate which subsequently reduces the uncertainty by a factor of $\sqrt{2}$.

In the course of the 3 days of measurements, many PNAR Ratios were calculated. Each PNAR Ratio involved two approximately 120 second counting periods; one period with

the Cd liner near the detectors ond one with it far away. Each of these 120 second periods were divided into 15 second counting intervals; thus there were generally 8 separate counting intervals. This division of counting periods into smaller intervals allowed for studying the statistical fluctuations in more detail. However, after each 15 second interval, a few seconds were lost, cumulatively increasing the total time of each measurement to 3 minutes.

In all examined cases, calculating the sample standard deviation of the 8 subsequent counting intervals, resulted into smaller standard deviation estimate than by taking the square root of the total counts. Another example of the difference between the two uncertainty estimations was evident when 114 measurements each lasting 15 seconds were made in row for a stationary assembly. 73 of the 114 measurements, or 64%, were within one standard deviation of the mean when the standard deviation was calculated from the variation in the counting intervals. Yet, when the standard deviation was estimated by taking the square root of the total counts; hence, assuming a Poisson distribution, 95 of the 114 points, or 83%, were within one standard deviation. If the counting statistics ever becomes the major source of error, dividing the counting period into smaller intervals can be beneficial, especially if the total measurement time can be kept close to 120 seconds with better software.

3.2.2 Repeated measurements

A total of 6 different assemblies were measured more than once from the default measurement height. Assemblies #4 and #1 were re-measured after the assemblies were once returned to the storage racks. Assemblies #18, #24, #28 and #42 were rotated four times by 90 degrees between measurements resulting into 5 independent measurements. Additionally, assembly #28 was measured 2 extra times from the default position. Both times, it was re-picked from the storage rack.

The pooled variance method can be used to estimate the standard deviation of the PNAR Ratio using three different subsets of these 26 measurements. Each calculation assumes that the underlying positioning uncertainty is the same for all assemblies in the subset.

1. Using one of each rotation angle of the four rotated assemblies (16 data points) the estimate for absolute standard deviation is 0.0013. This method averages over any rotational asymmetries in the fuel.

2. Using only the default measurement orientations (14 data points) yields an estimate of standard deviation of 0.0007.

3. Using all the 26 data points results into standard deviation estimate of 0.0012. This set includes more measurements at the default orientation than at other angles. (i.e. the orientations are not equally weighted)

In all cases, the size of the error is in the same magnitude as the counting error of individual measurements. The deviations of the PNAR Ratios of each individual measurement from the mean of all measurements of the same assembly, are shown in

Figure 8. The red lines in the figure indicate one standard deviation of 0.0012. Each "rot#" indicates a 90 degree counter clockwise rotation after the previous measurement.

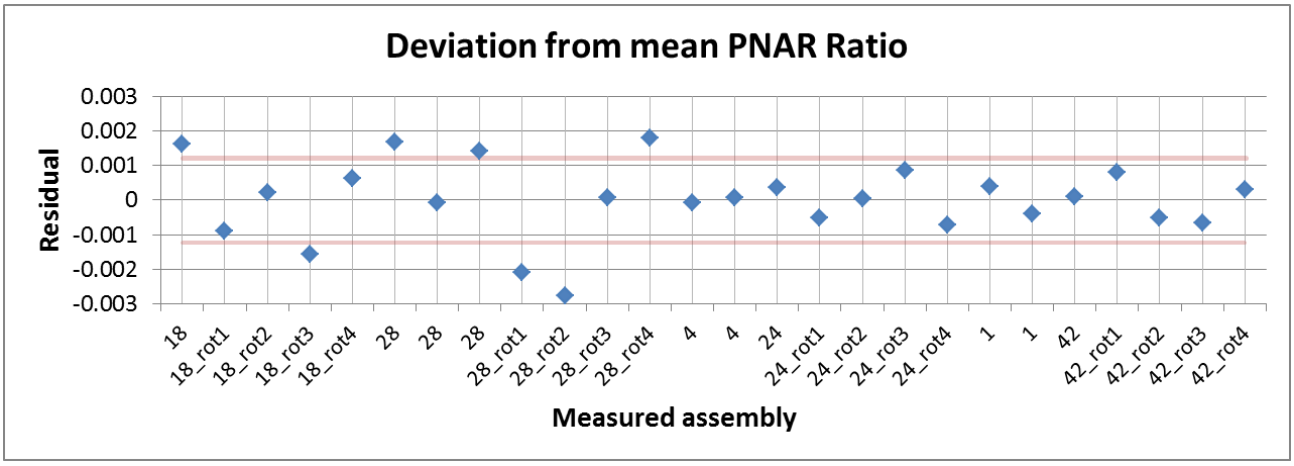

Figure 8: Deviation of PNAR Ratio of a single measurement from the mean of PNAR Ratios of all measurements of the same assembly. The red lines indicate one standard deviation calculated from these same 26 data points using the pooled variance method.

As the uncertainty caused by counting statistics also affects these measurements, the repositioning of fuel seems to not be a large source of uncertainty. However, it is still possible that the act of grappling and moving a fuel assembly would affect the positioning more than only rotating the assembly as most of the data points were from rotations. A series of measurements of same assembly while re-picking it from the storage rack and one rotation series is suggested for the next campaign. Measuring other assemblies in between would ensure that the repetitions are truly like any random inspection.

3.2.3 Vertical Cd liner offset

As the Cd liner was pulled up into the low-multiplying configuration and held there manually, the effect of the vertical position of the Cd liner was studied by gradually lowering the liner and measuring the count rate for 2 minutes at each liner location. The length was measured in chain links, which were approximately 2.4 cm apart. The resulting PNAR Ratios calculated from each measurement are presented in Figure 9. From a visual inspection of Figure 9, a small offset of up to 3 links does not appear to affect the PNAR Ratio. However, after that the effect is significant.

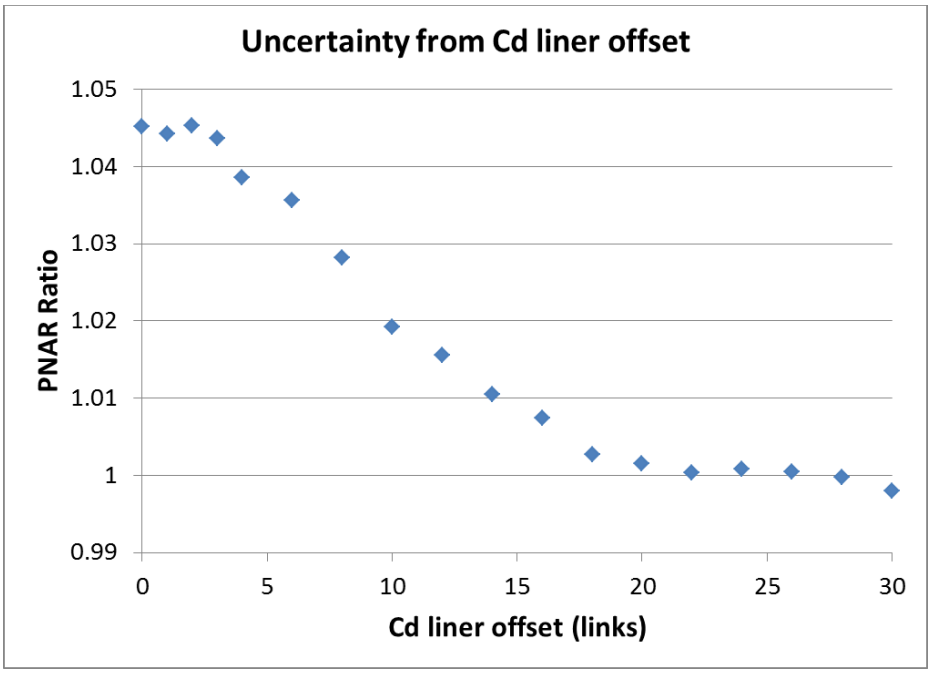

Figure 9: PNAR Ratio after lowering the Cd liner gradually from the default low-multiplying position. The distance between two chain links is approximately 2.4 cm.

4 Conclusions and discussion

The PNAR instrument functions within a safeguards system. The niche filled by the PNAR instrument within this system is to assure that the assembly is multiplying at a level consistent with the declared fuel assembly. The multiplication signature is unique compared to the other measured signatures as it assures that fissile material is present in the assembly. The other parts of the NDA system assure that fission fragments are present in every pin of the assembly (PGET) and that the total neutron count rate (a combination of the neutron source term and multiplication) and gross gamma intensity are consistent with the declaration (SCALE/MCNP). Together all of these measured signatures make the task of a would-be-proliferator very difficult.

Unlike the other signatures in the NDA system (gross gamma, total neutron, spatial location of photon emission) the PNAR signature does not change much from one typical assembly to the next. This constancy is to be expected and is a reflection that the reactor operator did a good job at optimally extracting the potential nuclear energy from each assembly. Assemblies arrive at a reactor with various initial enrichments. It is the task of the individuals that shuffle the fuel around the reactor to select locations in the reactor that optimally extract nuclear energy; hence, an assembly with a larger initial enrichment will be irradiated longer, or more intensely, typically. The constant among most all commercial assemblies is that the discharge multiplication of each assembly is very similar.

Steve Tobin

The PNAR instrument within the NDA System proposed by STUK is useful if it can achieve the following:

(a) The PNAR instrument is sensitive to multiplication to such a degree that the difference between a non-multiplying and a typically multiplying assembly is significantly large, enabling the absence of a significant fraction of the fissile material to be detected. Detecting gradations in multiplication among the typical assemblies is a plus.

(b) The PNAR signature strengthens the connection between the measured signatures and the declaration by providing another unique signature to compare.

(c) The PNAR signature makes the overall system more difficult to fool by making the would-be-proliferator leave an object after diversion of material that multiplies at the necessary level, in addition to emitting the necessary total neutrons, gross gammas and emit photons of the correct energy from the necessary spatial locations.

(d) The PNAR instrument is robust and of minimal burden to the nuclear facility operator and the safeguards agencies.

With respect to (a), a typical assembly has a PNAR Ratio of 1.044; a value obtained by average in the PNAR Ratios from

Table 3 excluding assembly #5 as, given its IE and BU values, is significantly under irradiated. The change in the PNAR Ratio from a non-multiplying assembly and a typical assembly is 1.0440 – 0.9800 or 0.0640. Given the estimated systematic uncertainty of 0.0012 estimated in Section 3.2.2, there are ~53 sigma of sensitivity between a non-multiplying assembly and a typical fully irradiated assembly.

One would hope that the PNAR Ratio can discern among fully irradiated assemblies. At a rough level, the current data indicates that this is possible as the one assembly that is most underirradiated, Assembly 5, has an elevated PNAR Ratio of 1.088 that is significantly above the average value of 1.044. However, with respect to discerning among the majority of the typically irradiated assembly, the current data is not particularly encouraging. Yet, a relevant point in this context is that axially specific, radiation history specific, simulations are needed given that the PNAR instrument only measures the multiplication from ~13% of the assembly in a single measurement and that the details of irradiation histories can make a significant difference. Yet, once such detailed simulations are done, the next research question becomes the accuracy of the simulations relative to the measurements. Fortunately, the resolution of this question is not central to the utility of PNAR within the overall NDA system (PGET, PNAR, ORIGEN/SCALE).

Point (b) will be the focus of research performed over the next half a year and the topic of a follow-up report. The authors suggest that point (c) is satisfied; yet measurements or simulations made to test the amount of the assembly that needs to be replaced before detection would help. Once the movement of the Cd liner is automated reliable, the instrument is anticipated to satisfy point (d).

Some issues that remain to be resolved include: (e) what axial location is best to measure or can this be a flexible choice with a different anticipated value at various axial locations? As seen from the pod-specific and axial PNAR Ratios, the PNAR Ratios one can measure from a single assembly are greatly affected by the choice of measurement position. Ultimately, this is caused by a complex distribution of fissile isotopes in the SNF affected by assembly type, pin design, position in core, void ratio etc. As the declared variables are typically average IE, average BU and cooling time, formulating a PNAR response function from only these data might turn out to be a difficult task. Using all four pods is a good way to simultaneously increase the counting efficiency and average the azimuthal variation.

Additionally (f) the degree to which different fuel types may follow different calibration curves may need to be resolved. The axial variation inspected in Section 3.1.2 hints that assembly type might affect the axial difference of PNAR measurements. Therefore, measuring from a lower height of the assembly might yield more easily interpretable results. In future campaigns, more axial scans from more than 2 heights should be considered to confirm this effect, including SVEA-64 assemblies. It may be possible that the variation with fuel type can be ignored by regulators if the difference is not too large.

Based on the repeated measurements, the effect of positional uncertainty seems very low. One reason could be that the centre channel was tighter than designed, which means that the fuel assembly position was well controlled. Furthermore, the movement

of the cadmium liner along the centre channel was very similar between measurements. The liner was pulled from one edge only which wedged the liner against the centre channel. This probably means that the liner had more freedom to move in the direction perpendicular to the lifting point. However, pods 2 and 4, used for most of the analysis, were the ones this movement would have affected. Nevertheless, the prototype performed better than expected in this regard.

5 Possible improvements

The following is a list of possible improvement to the PNAR Instrument:

a. Automate the movement of the Cd liner and a separate system that confirms the liner position.

b. Engineer the Cd-liner so that it bows in the opposite sense to its current bow, which has the liner most narrow at the ends and broadest in the middle. This would help in two ways: (a) the PNAR instrument would be more sensitive as the Cd liner in the most sensitive region of the liner, the region at the same axial height as the ^{3}He tubes, would be more able to reduce the multiplication in that region and (b) the Cd liner would have a greater mechanical tolerance at the crucial point where the liner needs to move over the central metal chamber.

6 References

[1] Tupasela Topi, Master's Thesis, *Passive neutron albedo reactivity assay of spent nuclear fuel,* 2019. Available online: http://urn.fi/URN:NBN:fi:aalto-201908254886

[2] Tobin, S. J., Peura, P., Honkamaa, T., Dendooven, P., Moring, M., and Bélanger-Champagne, C. *Passive neutron albedo reactivity in the Finnish encapsulation context,* Säteilyturvakeskus, 2017. Available online: http://www.julkari.fi/handle/10024/135811

7 Attachments

Pod-specific and total PNAR Ratios and gamma count rates of all measurements.

8 Appendix A: Data processing

As explained in Section 2, pod-specific counting data was collected in 15 second intervals. These intervals were not in sync between the pods. During the measurement campaign, the starting and ending time of each measurement was manually written down using the clock of the same computer that was running the counting software. The automated script to calculate the PNAR Ratios operates as follows.

1. All counting intervals that have started after the stated measurement start time and at least 15 second before the stated end time are collected for all detectors. The number of data points in this interval * 15s is the total measurement time. Because the detectors are not in sync with each other, the measurement time can differ between detectors in one measurement. To account for this, the counts are normalized to 1/s.

    a. Note that the measurement times varied between measurements because of the human element involved. Cd liner measurements tend to be shorter than non-Cd ones as the liner was manually held up. Some measurement times over lunch were very long compared to the average cases. All (detector specific) measurement times are saved in the output file.

2. The hand written measurement windows were validated manually by plotting the count series together with the measurement windows and visually checking that the cps was stable within the windows. The movement of assemblies and Cd liner was easily identifiable from the data. Figure 10 shows an extraction from the count series plot.

3. The data from measurements flagged as with Cd and without Cd measurements of the same assembly are aggregated together to create a single entry for each measurement pair.

4. Pod-specific and average PNAR Ratios are calculated from the count rates. The associated uncertainties are calculated using the total counts.

5. The end result is the excel file attached to this document. It contains PNAR Ratios for each detector, together with detector specific counting times and count rates, PNAR Ratios for the detector pair 2 and 4 and for all 3 detectors combined and gamma count rates for both with Cd liner and without Cd liner measurements. Assembly parameters were added to the table.

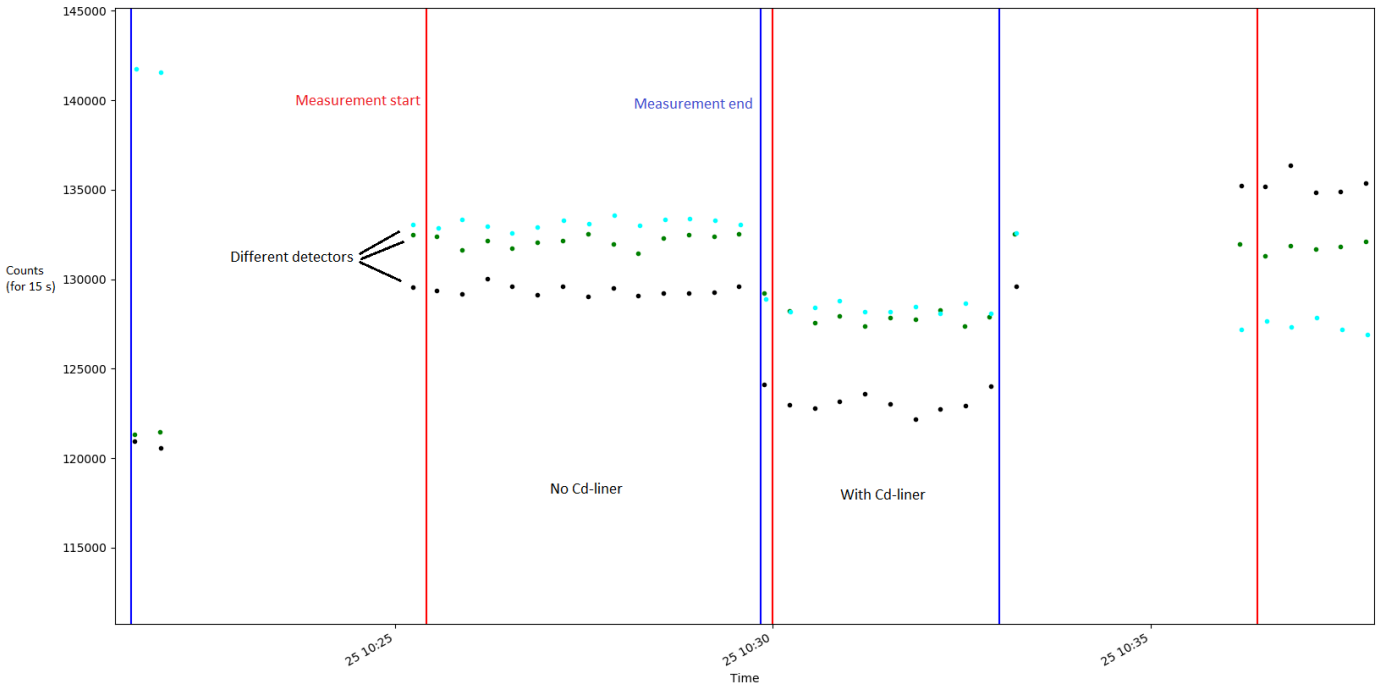

Figure 10: Example of collected measurement data (points) together with measurement start times (red) and end times (blue). The last data points of the "With Cd-liner"-measurement are not included in the data analysis, as they are located <15s from the measurement end time and thus, can contain counts from when the Cd liner was released or/and the fuel was moving.